

A CBXFEL DEMONSTRATOR SETUP AT THE EUROPEAN XFEL *

I. Bahns[†], S. Casalbuoni, M. Dommach, M. Di Felice, W. Freund, B. Friedrich, J. Grünert, S. Karabekyan, A. Koch, D. La Civita, L. Samoylova, H. Sinn, K. Tasca, M. Vannoni

European XFEL GmbH, Schenefeld, Germany

P. Rauer[‡], W. Decking, D. Lipka, T. Wohlenberg

Deutsches Elektronen-Synchrotron DESY, Germany

W. Hillert, J. Rossbach

Universität Hamburg, Hamburg, Germany

Abstract

A cavity based free-electron laser (CBXFEL) is a next generation X-ray source promising radiation with full three-dimensional coherence, nearly constant pulse to pulse stability and more than an order of magnitude higher spectral flux compared to self-amplified spontaneous emission (SASE) free-electron lasers (FELs). In this contribution, an R&D project for installation of a CBXFEL demonstrator experiment at the European XFEL facility is conceptually presented. It is composed of an X-ray cavity design in backscattering geometry of 133 m round-trip length with four undulator sections of 20 m total length producing the FEL radiation. It uses cryocooled diamond crystals and employs the concept of retroreflection to reduce the sensitivity to vibrations. The current state of the project shall be presented in this contribution.

INTRODUCTION

Current hard X-ray XFEL machines, such as the Linac Coherent Light Source (LCLS), the European XFEL (EuXFEL), the Spring-8 Angstrom Compact free-electron Laser (SACLA), the SwissFEL and the Pohang Accelerator Laboratory X-ray Free Electron Laser (PAL-XFEL), mainly use the SASE scheme for operation. However, the SASE operation suffers from low monochromaticity and poor longitudinal coherence. To improve this, hard x-ray self-seeding (HXRSS) has been successfully implemented [1, 2], and Cavity Based X-ray FEL (CBXFEL) schemes like high gain X-ray Regenerative Amplifier FELs (XRAFEL) [3] and low gain X-ray Free Electron Laser Oscillators (XFEL) [4] have been proposed. CBXFELs have received growing interest due to their anticipated ability to deliver outstanding radiation properties. The European XFEL is developing a CBXFEL demonstrator to prove the working concept. The setup has a peak gain of ≤ 14 , and the first results are expected in 2024 [5]. Here, we will present the current state of this project.

* This work was funded by the Federal Ministry of Education and Research under FKZ 05K16GU4, by the European XFEL GmbH and by Deutsches Elektronen-Synchrotron (DESY)

[†] immo.bahns@xfel.eu

[‡] patrick.rauer@desy.de

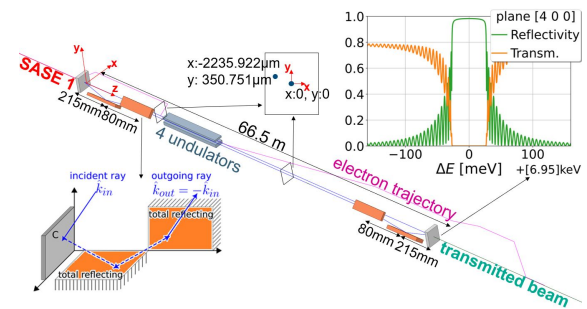


Figure 1: Conceptual design for the CBXFEL at the European XFEL. Considering the orientation of the retroreflector components and the illustrated z-spacing between the KB mirrors and the diamond crystal, the illustrated transverse (x-y-plane) position for a desired grazing incidence angle of 3.1 mrad can be calculated. Using retroreflector properties, the incoming direction is set to be antiparallel to the outgoing direction. The diamond Bragg reflector in C400 orientation has a very narrow bandwidth of about 20 meV around 6.95 keV. The reflected photons in this bandwidth are used for electron bunch seeding, and the photons outside the bandwidth are transmitted if not absorbed in the 100 μm thick crystal.

CONCEPTUAL DESIGN FOR THE CBXFEL AT EUROPEAN XFEL

In Fig. 1, a sketch of the conceptual design of the CBXFEL setup is illustrated. The setup is planned to be installed in the XTD2 tunnel at the end of the SASE1 undulator section at the European XFEL. The desired round-trip length of the X-ray cavity is determined by the electron bunch repetition rate. At the EuXFEL, the repetition rate is most commonly set to the 576th harmonic $f_{\text{rep}} = \frac{f_{\text{MO}}}{576} \approx 2.25 \text{ MHz}$ of the $f_{\text{MO}} = 1.3 \text{ GHz}$ base frequency of the master oscillator (MO) of the RF-cavities. For the CBXFEL this yields a photon round-trip time of 443 ns and corresponds to a round-trip length of 133 m. The exact value of the master oscillator frequency can be measured so precise that the length of the cavity can be predefined with μm precision. The FEL radiation inside the cavity is produced in four undulator segments of 20 m active length. The cavity employs the concept of retroreflection to reduce the sensitivity to vibrations and enhance the angular stability during alignment. Each retroreflector consists of a diamond Bragg reflector in backscattering

orientation and two silicon mirrors with B4C coating in Kirkpatrick–Baez (KB) geometry. The KB mirrors are also used for focusing. The choice of the C400 reflection order of the Bragg reflector sets the seeding photon energy to 6.95 keV. To ensure high reflectivity (>99%) and low clipping of the radiation at the finite size KB mirrors, the desired range for grazing incidence angles at the mirrors is in the range between 3 mrad to 4 mrad. By defining the exact values for the incident angles and the orientation of the retroreflector components in Fig. 1, unique transverse positions of the photons along their path can be determined.

The position of the vacuum chamber illustrated in Fig. 2 can be pre-aligned in the tunnel with an accuracy of about 300 μm by using a geodetic measuring method. The position of the holder of the KB mirrors and diamond crystals with reference to the vacuum chamber can be measured with a tactile 3D-measurement system. This pre-alignment is expected to determine the positions of the cavity components with a tolerance less than 1 mm. To do precise alignment of the cavity to the desired transverse positions, a stepwise alignment approach by observing the beam position on scintillators as illustrated in Fig. 2 can be used. To achieve this alignment, the diamond crystals and the KB mirrors can be rotated around and translated along the x-axis and y-axis (using the axis definition of Fig. 1), using positioning stages based on the concept of parallel kinematics [6]. Since no remote alignment involving rotations around the z-axis is planned, possible differences between both retroreflectors and the KB mirrors inside each retroreflector are set by the pre-alignment. The pre-alignment between the KB mirrors is planned to be adjusted with sub-mrad precision with an autocollimator. The rotation between both retroreflectors is set by the before mentioned pre-alignment method in combination with a tactile 3D-measurement system and might be in the range of a few mrad. However, the errors introduced by differences in this range can be compensated by proper choice of grazing incidence angles, so that the retroreflecting properties are preserved.

Applying this alignment scheme, a closed trajectory for the reflected X-ray photons can be achieved. The transverse position can be aligned with μm precision of. Following simulations, this yields a transverse overlap between electron bunch and reflected photon pulse (in the x-y-plane referred to the coordinate system shown in Fig. 1) to reach sufficient gain in the cavity to overcome the losses.

After successful transverse alignment, a grating in the diagnostic chamber can be inserted into the beam instead of the scintillator, as illustrated in Fig. 3. The pulse energy of the first diffraction order beam will be measured with a photodiode. Monitoring the decrease of the pulse energy with each round-trip will give important insights to the cavity losses, and, hence, to the quality of the X-ray optics components. This ring-down measurement will yield an experimental demonstration of a large-scale x-ray laser cavity, similar to the experiment recently done at LCLS [7] and can be seen as an important milestone for the commissioning of the CBXFEL demonstrator project.

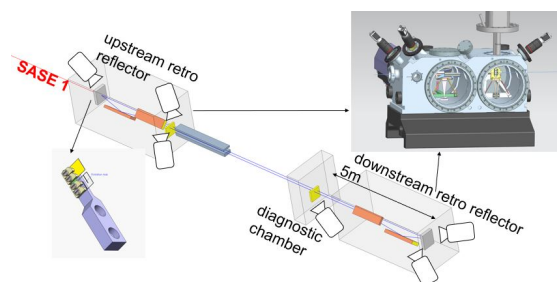


Figure 2: Sketch of diagnostics to measure the beam positions. In the cavity, the beam positions can be measured at six different positions using YAG scintillators in combination with cameras to achieve μm spatial resolution. The gray boxes in this sketch indicate which components are placed in the same vacuum chamber. In the upstream retroreflector vacuum chamber also a scintillator is present, whereas for the downstream retroreflector a separate diagnostic vacuum chamber is placed 5 m apart to measure the beam direction after reflection. The beam position can also be monitored at the yellow marked side face of the KB mirrors. Additionally, the diamond crystals can be replaced by a scintillator during operation for alignment purposes.

The next step is to achieve longitudinal overlap. To achieve a well-defined overlap between the photon pulse and the electron bunch, the repetition rate of the electron bunch should match the photon round-trip time within a range of 40 fs. This corresponds to an alignment tolerance of 5 μm of the distance between the retroreflectors. To achieve this alignment, the complete downstream retroreflector vacuum chamber illustrated in Fig. 2 can be translated in z-direction to the desired position. The retroreflecting scheme of the optical elements compensates for any parasitic motion of this travel and should allow maintaining the transversal alignment while adjusting the cavity length. If there is both transverse and longitudinal overlap, with the prior being ensured by the transverse alignment and the ringdown measurement, an exponential increase in the pulse energy is expected, as illustrated in Fig. 4. Observing an exponential increase of the pulse energy will confirm that the CBXFEL principle is working, and, hence, is the main goal of this demonstrator project. For monitoring this seeding process, two different options are available. The first is the grating in combination with a photodiode as illustrated in Fig. 3 and the second is the pulse resolved HIGH RESolution hard X-ray single-shot (HIREX) spectrometer installed further downstream in the SASE1 beamline [8].

Another promising method for the longitudinal alignment is the use of a pulse arrival time chirp [9, 10]. Introducing an arrival time chirp on the order of about 1 ps over a pulse train enables the longitudinal scanning for seeding with a much relaxed tolerance of hundreds of μm per mechanical translation of the downstream chamber.

Using cryogenic cooling for the diamond Bragg reflectors is a common attempt to improve the cavity's stability by better distributing the pulsed heat load given by the interac-

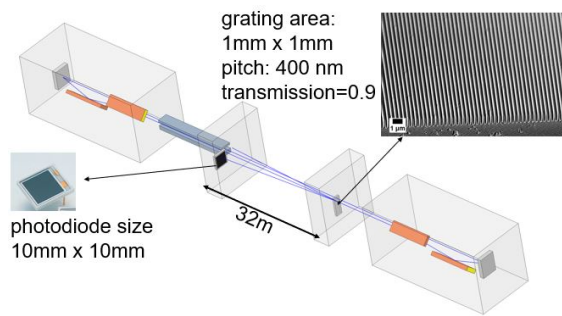


Figure 3: A diamond grating fabricated on a $80\text{ }\mu\text{m}$ thick diamond substrate can be used to diffract a part of the pulse energy after the reflection at the downstream retroreflector on to a photodiode. The grating is placed on a remotely controllable linear manipulator, which is also used for the scintillator inside the diagnostic chamber illustrated in Fig. 2.

tion of the Bragg reflector with the powerful X-ray pulses. Pulsed cryogenic coolers are also planned to be installed for the CBXFEL demonstrator. Our simulations [5] revealed that due to cryogenic cooling, a significant increase of the out coupled pulse energy by about a factor of 30 is expected. Monitoring the significant increase of pulse energy due to cryogenic cooling is another important milestone for the demonstrator project. Nevertheless, due to the high heat load on the $100\text{ }\mu\text{m}$ thin crystals, stable operation under saturation is not expected for our current demonstrator project.

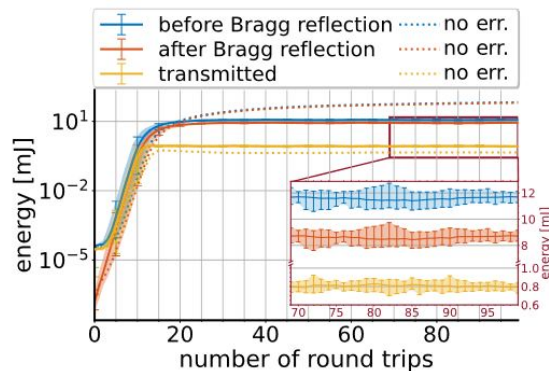


Figure 4: Results of start to end simulations, which take account of realistic electron bunch distributions, inter RF-pulse bunch fluctuations and various possible errors of the X-ray optics. Heat load effects were excluded in this simulation. For further details, see Ref. [5].

Detailed information regarding the simulation framework used to calculate the results in Fig. 4 can be found in one of our recent publications [5]. Figure 4 indicates that even for a simulation considering realistic roughness of the X-ray optics and jitter of the electron beam, stable operation of a

CBXFEL seems to be feasible, which enables out-coupling of X-ray pulses with a very narrow bandwidth of hundreds of meV. However, as mentioned before, due to heat load effects, stable operation is not expected for the demonstrator CBXFEL. After the successful commissioning of the CBXFEL, which is planned for summer 2024, the next step may be an upgrade of the demonstrator with thick diamond crystals and out-coupling via a grating. Thicker crystals could improve the stability of the diamond Bragg reflectors under dynamic heat load [11] and may be considered as an interesting pathway towards finally reaching stable operation under saturation.

REFERENCES

- [1] S. Liu *et al.*, “Cascaded hard X-ray self-seeded free-electron laser at MHz-repetition-rate”, *Preprint*, Jan. 2023. doi:10.21203/rs.3.rs-2487501/v1
- [2] J. Amann *et al.*, “Demonstration of self-seeding in a hard-X-ray free-electron laser”, *Nat. Photonics*, vol. 6, p. 693, Aug. 2012. doi:10.1038/nphoton.2012.180
- [3] Z. Huang and R. D. Ruth, “Fully Coherent X-Ray Pulses from a Regenerative-Amplifier Free-Electron Laser”, *Phys. Rev. Lett.*, vol. 96, no. 14, p. 144801, Apr. 2006. doi:10.1103/PhysRevLett.96.144801
- [4] K.-J. Kim, Y. Shvyd’ko, and S. Reiche, “A Proposal for an X-Ray Free-Electron Laser Oscillator with an Energy-Recovery Linac”, *Phys. Rev. Lett.*, vol. 100, no. 24, p. 244802, Jun. 2008. doi:10.1103/PhysRevLett.100.244802
- [5] P. Rauer, *et al.*, “Cavity based x-ray free electron laser demonstrator at the European X-ray Free Electron Laser facility”, *Phys. Rev. Accel. Beams*, vol. 26, no. 2, p. 020701, Feb. 2023. doi:10.1103/PhysRevAccelBeams.26.020701
- [6] T. Noll *et al.*, “Parallel kinematics for nanoscale Cartesian motions”, *Precision Engineering*, vol. 33, no. 3, p. 291-304, Jul. 2008. doi:10.1016/j.precisioneng.2008.07.001
- [7] R. Margraf *et al.*, “Low-loss Stable Storage of X-ray Free Electron Laser Pulses in a 14 m Rectangular Bragg Cavity”, *Preprint*, Jan. 2023. doi:10.21203/rs.3.rs-2465216/v1
- [8] N. Kujala *et al.*, “Hard x-ray single-shot spectrometer at the European X-ray Free-Electron Laser”, *Rev. Sci. Instrum.*, vol. 91, no. 10, p. 103101, Oct. 2020. doi:10.1063/5.0019935
- [9] M. K. Czwalińska *et al.*, “Beam Arrival Stability at the European XFEL”, in *Proc. IPAC’21*, Campinas, Brazil, May 2021, pp. 3714–3719. doi:10.18429/JACoW-IPAC2021-THXB02
- [10] M. Diomedea *et al.*, “Update on the LLRF operations status at the European XFEL”, in *LLRF Workshop 2022 (LLRF2022)*, 2022. doi:10.48550/arXiv.2210.04711
- [11] I. Bahns *et al.*, “Stability of Bragg reflectors under megahertz heat load at XFELs”, *J. Synchrotron Radiat.*, vol. 30, no. 1, pp. 1–10, Jan. 2023. doi:10.1107/S1600577522009778